Surface Science 656 (2017) 1–6

Contents lists available at ScienceDirect

Surface Science

journal homepage: www.elsevier.com/locate/susc

C_{70} self-assembly on In- and Tl-adsorbed Si(111)$\sqrt{3} \times \sqrt{3}$-Au surfaces

D.A. Olyanich[a,b], V.V. Mararov[a,b], T.V. Utas[a,b], A.V. Zotov[a,b,c,*], A.A. Saranin[a,b]

[a] *Institute of Automation and Control Processes FEB RAS, 5 Radio Street, 690041 Vladivostok, Russia*
[b] *School of Natural Sciences, Far Eastern Federal University, 690950 Vladivostok, Russia*
[c] *Department of Electronics, Vladivostok State University of Economics and Service, 690600 Vladivostok, Russia*

ARTICLE INFO

Keywords:
Molecular–solid interactions
Silicon
Fullerene
Self–assembly
Adsorption
Scanning tunneling microscopy

ABSTRACT

Behavior of C_{70} fullerenes adsorbed onto the In- and Tl-modified Si(111)$\sqrt{3} \times \sqrt{3}$-Au surfaces at room temperature (RT) and 112 K has been studied using scanning tunneling microscopy observations and compared with the known results for the C_{60}s on the same surfaces. During island growth at 112 K, both C_{70} and C_{60} are characterized by the same critical island size i=1. The difference is in an island shape as C_{70}s tend to form chain-like islands built of double or triple molecular rows along the $[\bar{1}10]$ Si(111) substrate directions. At RT, C_{70}s have a lower mobility as compared to C_{60}s. In contrast to the C_{60} magic islands, the C_{70} islands do not demonstrate any strong preference for specific shapes or sizes. Extended C_{70} arrays exhibit a stripe-like 3×1 reconstruction where a single row of bright fullerenes mediated by a double row of dim fullerenes. The reconstruction is due to the different orientations of C_{70}s within the layer which does not relate to the structure of the underlying Au/Si(111) substrate. This is in contrast to the hexagonal reconstructions of C_{60}s where the bright fullerenes occupy the specific adsorption site atop Au trimers. The difference in the behavior of C_{70} and C_{60} is plausibly affected by the non-spherical shape of C_{70} molecule and a greater intermolecular C_{70}-C_{70} interaction.

1. Introduction

The adsorption of fullerenes onto metal and semiconductor surfaces has attracted considerable interest due to a variety of the fascinating phenomena underlying fullerene self-assembly. Among such phenomena one can mention developing modulations in the close-packed fullerene monolayers which shows up as appearance of molecules having two different contrast in scanning tunneling microscopy (STM) images: "bright" and "dim". The bright-dim contrast was observed in C_{60} monolayers on many noble-metal surfaces, including Ag(111) [1,2], Ag(100) [3–5], Au(111) [6–9], Cu(111) [10], Cu(100) [11]. The apparent height difference between bright and dim molecules can amount to ~1–2 Å. However, the origin of this contrast remains a debated subject as it can result from the electronic effects, the molecular orientations, or the geometric effects due to substrate reconstruction. As for the metal/silicon surface phases, i.e. surface reconstructions induced by adsorption of metal submonolayers onto Si crystalline substrates, the distinct dim-bright contrast was observed in the C_{60} monolayers on the pristine Si(111)$\sqrt{3} \times \sqrt{3}$-Ag surface [12,13] and Si(111)$\sqrt{3} \times \sqrt{3}$-Au surface modified by In [14,15] or Tl [16] adsorption. In particular, the dim fullerenes in the C_{60} monolayers on Si(111)$\sqrt{3} \times \sqrt{3}$-Ag constitute ~10% of all fullerenes and reside ~1.6 Å lower than other fullerenes. It was suggested that formation of the dim C_{60} is associated with a disintegration of Ag trimer of Si(111)$\sqrt{3} \times \sqrt{3}$-Ag surface beneath a given fullerene [13]. In the C_{60} monolayers on the In- or Tl-adsorbed Si(111)$\sqrt{3} \times \sqrt{3}$-Au surfaces, the bright fullerenes are arranged in the well-defined two-dimensional (2D) lattices [14,16]. Note that adsorption of ~0.1–0.2 ML of In or Tl onto Si(111)$\sqrt{3} \times \sqrt{3}$-Au was used to remove domain walls, characteristic of the pristine surface [17], and to produce almost defect-free highly-ordered and homogeneous Si(111)$\sqrt{3} \times \sqrt{3}$-Au surfaces [18–20]. These surfaces preserve atomic arrangement of the pristine surface [21] but contains also a 2D gas of In or Tl adatoms. The bright C_{60} on these surfaces were recognized to reside directly atop the Au trimers, the most energetically unfavorable adsorption sites [14,15]. This fact has a remarkable sequence for the C_{60} island growth leading to size selection and magic C_{60} island formation. For example, more than 80 % of C_{60} islands grown on In-adsorbed Si(111)$\sqrt{3} \times \sqrt{3}$-Au surface can have identical shape and size, namely each contains 37 fullerenes arranged in a regular hexagon [15]. Bearing in mind this advantageous property of the particular fullerene-substrate pair, it seemed of interest to explore how changing of the spherical fullerenes C_{60} for the elongated fullerenes C_{70} would affect their growth mode. It is worth noting, however, that in many adsorption phenomena, C_{70} differ from C_{60} not only by the size and shape but rather by the different charge transfer [22], kinetic characteristics [23] and intermolecular interaction [24].

---

[*] Corresponding author at: Institute of Automation and Control Processes FEB RAS, 5 Radio Street, 690041 Vladivostok, Russia.
E-mail address: zotov@iacp.dvo.ru (A.V. Zotov).

http://dx.doi.org/10.1016/j.susc.2016.09.005
Received 1 August 2016; Received in revised form 20 September 2016; Accepted 21 September 2016

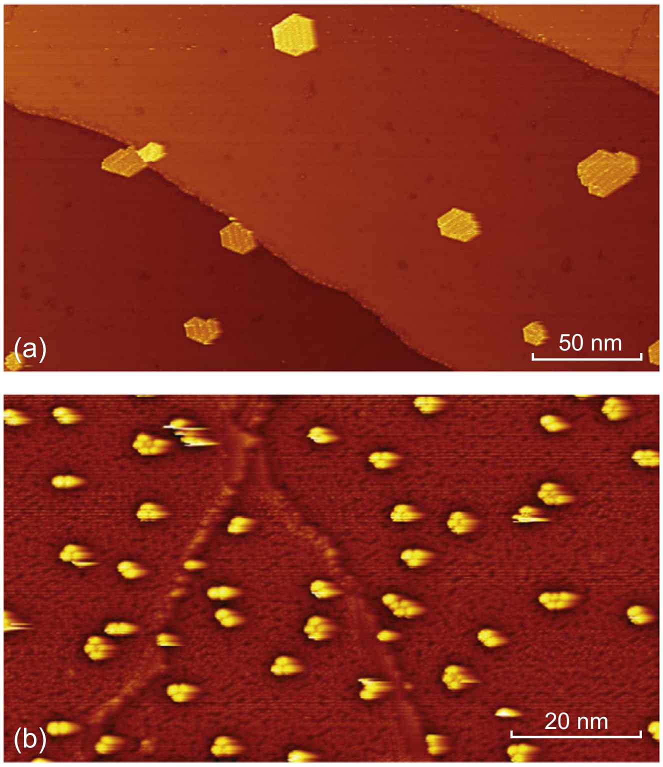

Fig. 1. STM images illustrating early stage of C_{70} island growth on In-adsorbed Si(111)$\sqrt{3} \times \sqrt{3}$-Au held at (a) RT and (b) 112 K. Scale: (a) 300 × 165 nm^2, (b) 100 × 55 nm^2.

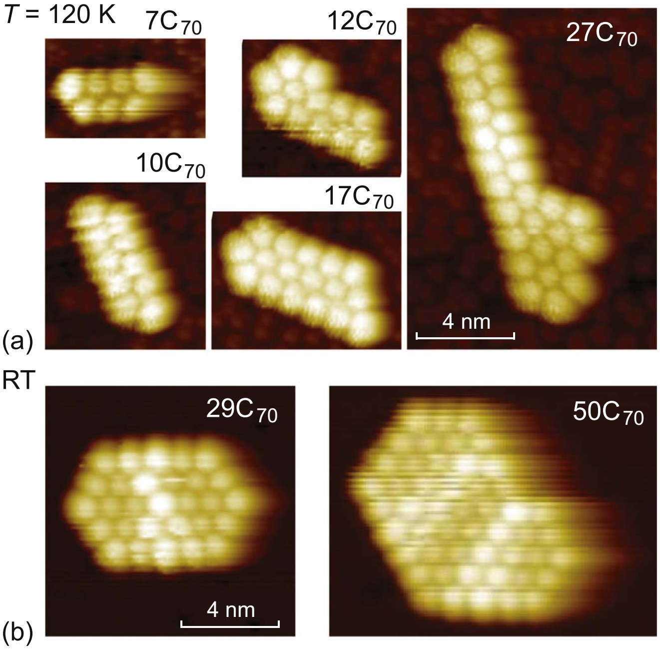

Fig. 3. Selection of C_{70} islands grown at (a) 112 K and (b) RT.

In the present paper, we report on the results of the STM study of C_{70} adsorption and self-assembly on In- and Tl-adsorbed Si(111)$\sqrt{3} \times \sqrt{3}$-Au surface which results are compared with those reported for C_{60} on the same surfaces. It has been found that non-spherical shape of C_{70} alters significantly the growth mode. Starting from the early stages, the islands tend to adopt elongated shapes. In the extended arrays, the molecules are arranged in the linear superstructure with alternating sequence of bright and dim C_{70} rows, namely one bright row is typically mediated by two dim rows. The superstructure does not demonstrate a clear resemblance with the structure of the underlying Au/Si(111) substrate and is plausibly a result of the interactions between molecule in various orientations.

2. Experiment

Our experiments were performed with an Omicron VT-STM operating in an ultrahigh vacuum (~2.0 × 10^{-10} Torr). Atomically-clean Si(111)7 × 7 surfaces were prepared *in situ* by flashing to 1280° C after the samples were first outgassed at 600° C for several hours. Gold was deposited from an Au-wrapped tungsten filament, indium and thallium from the Ta crucibles and fullerenes, C_{70} (BuckyUSA, purity 99.5%), from a resistively heated Ta boat. For STM observations, electrochemically etched tungsten tips cleaned by *in situ* heating were employed. To prepare the In- or Tl-modified Si(111)$\sqrt{3} \times \sqrt{3}$-Au surfaces, the Si(111)$\sqrt{3} \times \sqrt{3}$-Au surface was first formed by Au deposition onto Si(111)7 × 7 surface held at 600° C and then ~0.5 ML of In or Tl was

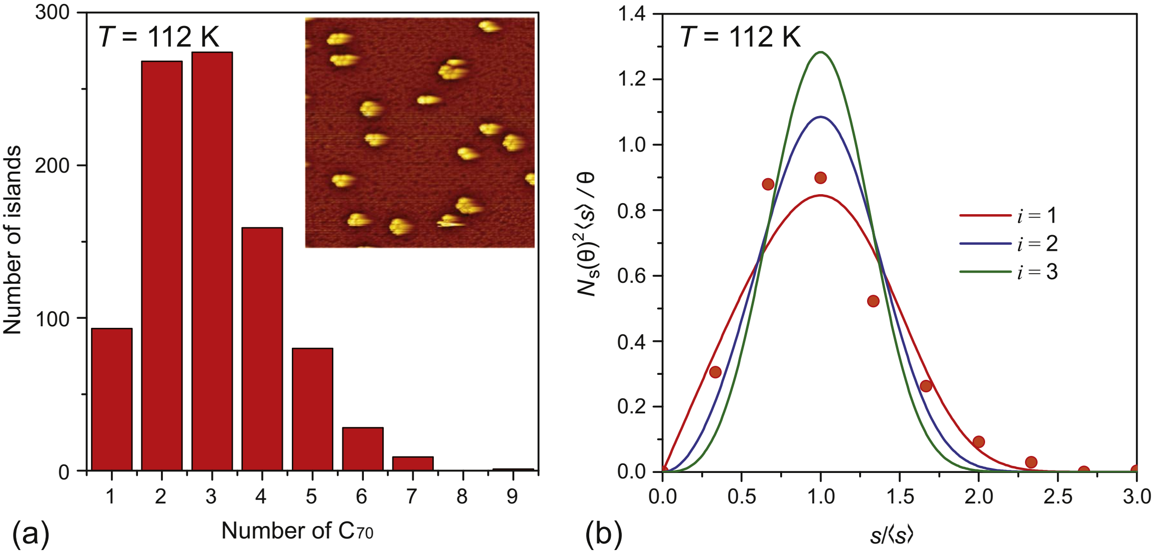

Fig. 2. (a) Experimental C_{70} island size distribution at 112 K. Inset shows a fragment of the surface with C_{70} island array under consideration. (b) Experimental scaled island size distribution (red circles) superposed on the simulated scaling functions f_i for critical island size i=1, 2, and 3 (red, blue and green lines, respectively). (For interpretation of the references to color in this figure legend, the reader is referred to the web version of this article.)

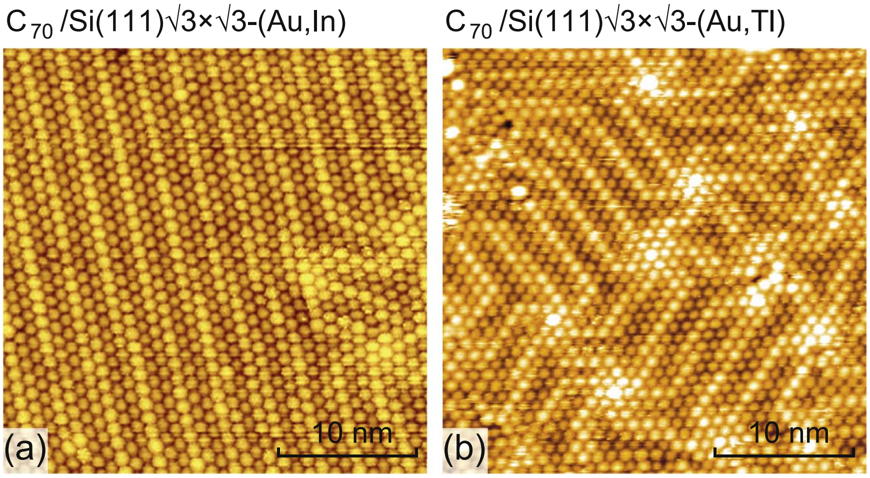

Fig. 4. $30 \times 30\ \mathrm{nm}^2$ STM images of C_{70} arrays grown on (a) In-adsorbed and (b) Tl-adsorbed $\mathrm{Si}(111)\sqrt{3}\times\sqrt{3}$-Au surfaces at RT.

deposited onto this surface held at room temperature (RT) followed by brief (∼15 s) annealing at ∼600° C for In and ∼350° C for Tl.

3. Results and discussion

First of all we would like to remark that the main regularities of C_{70} adsorption and layer growth were the same for both In- and Tl-adsorbed $\mathrm{Si}(111)\sqrt{3}\times\sqrt{3}$-Au surfaces. Fig. 1 illustrates the early stage of C_{70} layer growth at RT. Formation of the scarce islands indicates that C_{70} molecules demonstrate a relatively high mobility. However, nucleation of islands not only at the step edges but also at the terraces yields a rough estimation of diffusion length on the order ∼50–100 nm. This is lower than the corresponding value for RT migration of C_{60} on the same surfaces, where islands nucleate exclusively at the step edges even when the terraces are more than 100 nm in width. Note that a slower migration of C_{70} as compared to C_{60} can be thought as a general trend as a sequence of the difference in the molecule shape. In particular, the same rule was found to hold for the migration of C_{60} and C_{70} on $\mathrm{Si}(111)\sqrt{3}\times\sqrt{3}$-Ag surface [23]. The lower mobility of C_{70} molecules can be attributed to their non-spherical shape bearing in mind that rolling is rather typical for fullerene motion on surfaces.

When adsorption of C_{70} takes place at low temperature of 112 K, fullerenes agglomerate into molecular islands at terraces with island density of $\sim(0.5-1.0)\times10^{-2}\ \mathrm{nm}^{-2}$, hence the mean distance between islands is on the order of ∼10 nm. Fig. 1b shows STM image of such an array and Fig. 2a presents its island size distribution. These data can be processed using the scaling relation [25,26], $N_s = \Theta\langle s\rangle^{-2} f_i\,(s/\langle s\rangle)$, where N_s is the density of islands of size s (the number of molecules in the island), Θ is the coverage of adsorbate, $\langle s\rangle$ is the average island size, and f_i is the scaling function for the island size distribution for a critical island size i. Plotting $N\,(s/\langle s\rangle)\langle s\rangle^2\Theta^{-1}$ versus $s/\langle s\rangle$ (that essentially yields the experimental scaling function f_i) and comparing it with the simulated scaling functions, one can determine the size of critical island i. Such an evaluation is illustrated in Fig. 2b. One can see that the experimental data fit the simulated f_i plot for i=1. Remind that critical island size i is defined as the minimal size when the addition of just one more molecule makes the island stable. Hence, C_{70} dimer on the In- or Tl-adsorbed $\mathrm{Si}(111)\sqrt{3}\times\sqrt{3}$-Au surfaces is already a stable island which is the same as reported for the C_{60} molecules [27,28]. It is worth noting that this is rather typical situation for fullerenes adsorbed onto the relatively inert surfaces [29,30], in which case the intermolecular interaction is greater than that of molecules with a substrate.

Peculiar feature of the C_{70} island arrays formed at 112 K is that a noticeable portion of the islands has a chain-like shape built of the double or triple molecular rows aligned along the main crystallographic directions of Si(111), $[\bar{1}10]$. Selected examples of such islands are presented in Fig. 3a. When the islands are grown by C_{70} deposition at RT or by heating island arrays formed at 112 K to RT, the islands adopt generally a more compact shape (Fig. 3b). No noticeable preference for any specific island sizes and shapes are observed that is in contrast to the C_{60} fullerenes which under the same conditions demonstrate a strong tendency towards the growth of islands of magic sizes and shapes [15,16]. Remind that in the latter case the island size selection is controlled by the hexagonal superlattices ($\sqrt{19}\times\sqrt{19}$ – R23.4° for (Au, In)/Si(111) and $\sqrt{7}\times\sqrt{7}$ – R19.1° for (Au, Tl)/Si(111)) formed by the bright C_{60} fullerenes which occupy the most energetically unfavorable adsorption sites atop the Au trimers.

In case of the C_{70} fullerenes, another type of the dim-bright patterns develops. Its motifs appear in the islands starting from the size of about 30 C_{70} fullerenes (Fig. 3b) and the pattern becomes well-defined in the extended C_{70} molecular arrays. Figs. 4a and b show such arrays formed on the In- or Tl-adsorbed $\mathrm{Si}(111)\sqrt{3}\times\sqrt{3}$-Au surfaces, respectively. The C_{70} layer displays a stripe-like 3 × 1 superstructure where single rows of the bright C_{70}s are mediated by double rows of dim C_{70}s. Following the notation proposed for the superstructured C_{60} monolayers on Cu(100) [11], the C_{70} superstructure can be defined as 1B2D since it has a one-bright-and-two-dim ordering sequence of molecular rows. The C_{60} monolayers on Cu(100) have a similar appearance in STM, albeit with the other ordering sequences, namely there are two phases, 2B1D and 1B1D [11]. However, in spite of an apparent similarity in STM appearance the driving force for developing striped superstructures in the two cases, C_{60} on Cu(100) and C_{70} on In- or Tl-adsorbed Au/Si(111) surfaces, is quite different. For C_{60} on Cu(100), it develops due to superposing of the close-packed C_{60} film on a substrate of a different symmetry. In the present case, both the Au/Si(111) substrate and the closed-packed C_{70} layer possess basic hexagonal symmetry and the striped superstructure develops in the molecular layer due to the non-spherical shape of C_{70} molecules.

Let us consider now the structural properties of the 1B2D C_{70} monolayer in a greater detail. The C_{70} rows are aligned along the $[\bar{1}10]$ directions of the Si(111) substrate. Hence, following the substrate symmetry there are three equivalent 120°-rotated domains. The 1B2D contrast between fullerene rows in STM images is the same at both, positive and negative, bias polarities. An apparent height difference between dim and bright fullerenes is 0.3 ± 0.1 Å in the case of C_{70} on In-adsorbed $\mathrm{Si}(111)\sqrt{3}\times\sqrt{3}$-Au surface. In the case of Tl-adsorbed surface, the contrast is somewhat higher, ∼0.5 Å, though all other features of the superstructures are the same. In the regions where three rotational domains intersect, the fullerenes have the greatest apparent height. Thus, they can be called "superbright" fullerenes by analogy with the superbright C_{60} molecules on Ag(111) [2]. Scanning tunneling spectroscopy measurements conducted on dim, bright and superbright

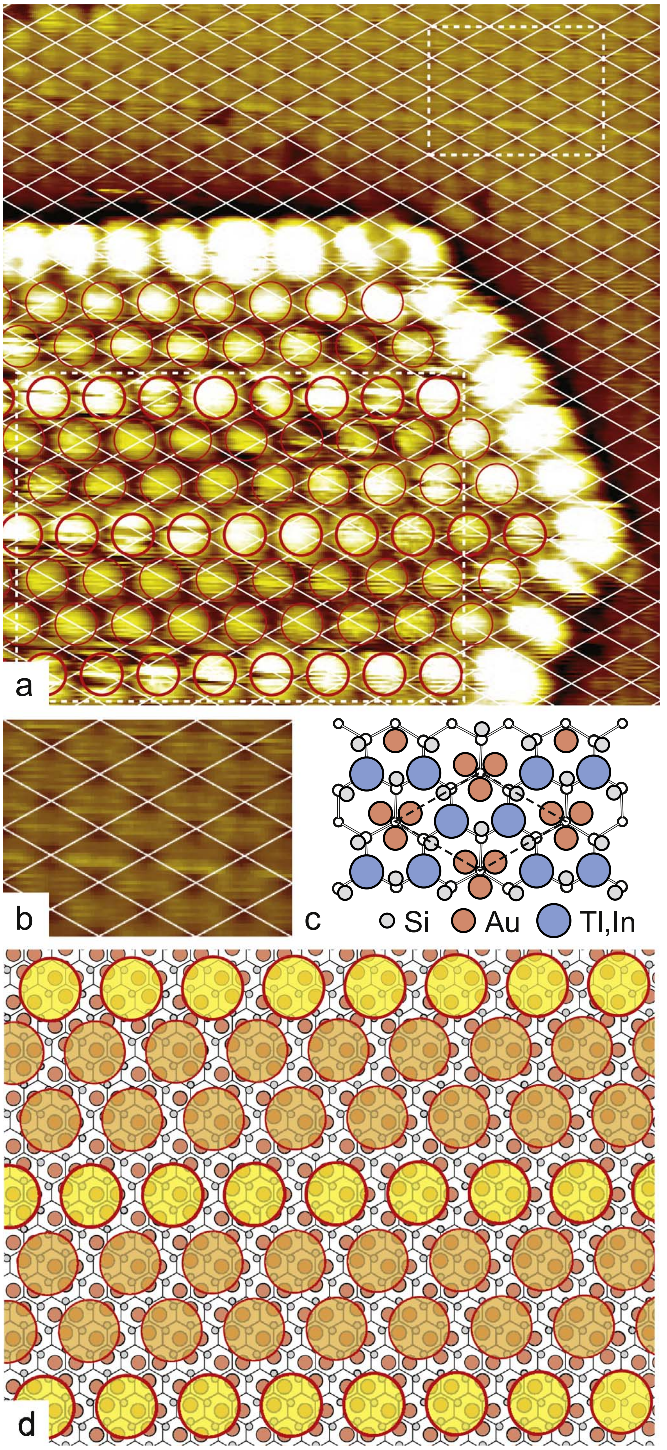

Fig. 5. Identification of the C_{70} adsorption sites within the molecular array. (a) STM image with coexisting C_{70} array and bare Si(111)$\sqrt{3} \times \sqrt{3}$-(Au, In) surface with the grid associated with the $\sqrt{3} \times \sqrt{3}$ periodicity. (b) Enlarged region of the Si(111)$\sqrt{3} \times \sqrt{3}$-(Au, In) surface outlined by the dashed frame in (a). (b) Schematics of the Si(111)$\sqrt{3} \times \sqrt{3}$-Au surface. Au trimers are shown by red circles, Si atoms by gray and white circles, blue circles indicate the adsorption sites of In or Tl atoms. The $\sqrt{3} \times \sqrt{3}$ unit cell is outlined to illustrate that depressions in (b) correspond to location of Au trimers [18,19]. (d) Schematics of the C_{70} array region outlined in (a) superposed on the structure of the underlying Si(111)$\sqrt{3} \times \sqrt{3}$-Au surface. Bright C_{70}s are shown by yellow circles, dim C_{70}s by orange circles. One can see that fullerene adsorption sites are random without any apparent difference between those for bright or dim fullerenes.

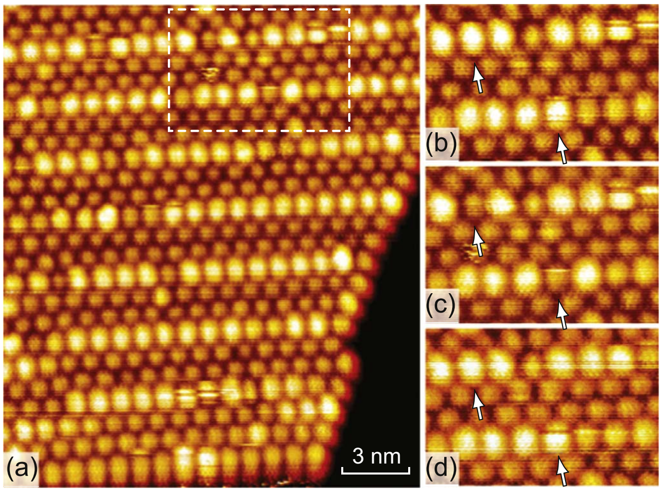

Fig. 6. (a) 19 × 22 nm^2 high-resolution STM image of the C_{70} array acquired at 112 K. (b), (c), and (d) Successive snapshots of the same fragment of the array where C_{70} molecules changing their appearance are indicated by arrows.

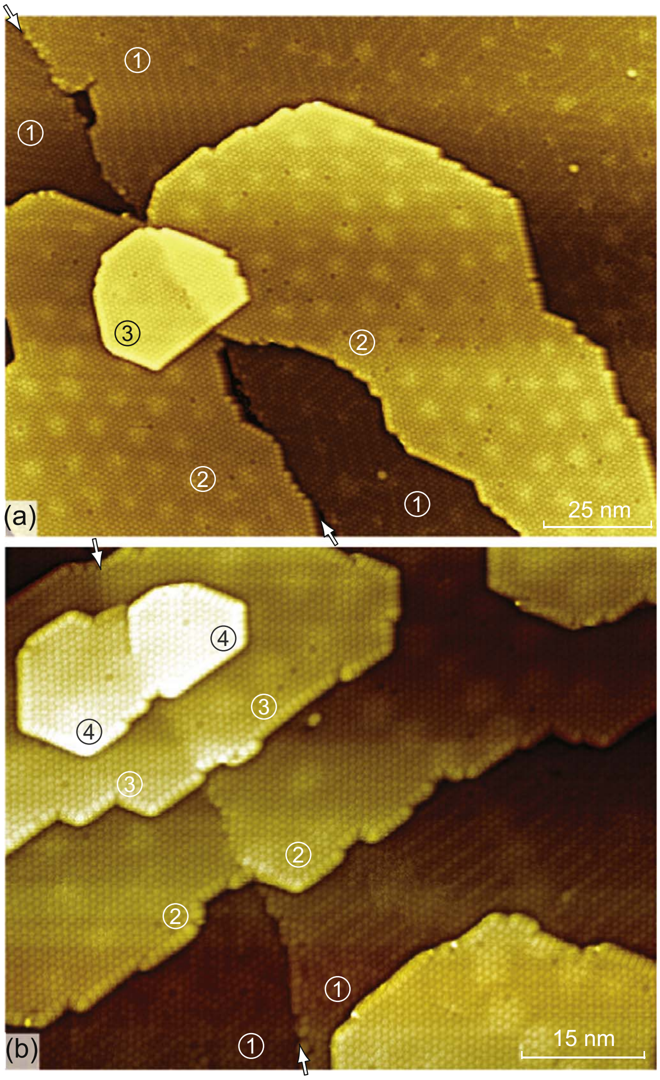

Fig. 7. 150 × 120 nm^2 STM image illustrating the onset of the third-layer island growth. (b) 85 × 66 nm^2 STM image showing the onset of the fourth layer formation. The numbers in circles indicate the layer number in the multi-layer systems. Arrows indicate the location of the atomic step at the Au/Si(111) substrate surface.

C_{70} molecules have revealed that their spectra are very similar. This imply that STM contrast is primarily due to topography. However, modest bias-dependent variation in apparent height difference is an indication that certain electronic effects cannot be completely excluded.

It is worth noting that the 1B2D superstructure of the C_{70} layers has no resemblance with the structure of the underlying Si(111)$\sqrt{3} \times \sqrt{3}$-Au surface. This is illustrated in Fig. 5 which shows that fullerenes occupy random sites without any apparent difference between those for bright or dim C_{70}s. This is contrasted with the C_{60} monolayers where the bright fullerenes are always those residing atop the Au trimers, while dim molecules are those occupying all the other adsorption sites. Thus, one can conclude that the role of the intermolecular interactions in the superstructure formation is prevailing for the C_{70} layers, plausibly due to a greater C_{70}-C_{70} binding as compared to the C_{60}-C_{60} one.

Fig. 6a shows a high-resolution STM image with a fragment of the 1B2D C_{70} array. One can see that dim C_{70}s have a round shape, while bright C_{70} have an oval shape with a long size oriented perpendicular to the direction of molecular row. This is in apparent contradiction with the expectation that bright fullerenes stand upright, while dim fullerenes lie on the surface. In turn, this implies that arrangement of C_{70} in the molecular layer is controlled by the more complicated mechanisms. For example, C_{70} molecules were suggested to tend to arrange in a configuration in which electron-poor regions on one molecule face electron-rich regions on the adjacent molecule [24]. It should be noted also that fullerenes in the C_{70} layer are in continuous rotation as evidenced by lacking of the intermolecular features characteristic of molecules in a fixed orientation. Moreover, the layer changes dynamically even at 112 K and selected bright C_{70}s transfer to dim C_{70}s and vice versa, as illustrated in Fig. 6b, c, and d.

With prolonged C_{70} deposition, almost the whole surface becomes occupied by the C_{70} monomolecular layer. Formation of the second-layer islands starts when more than 80% of the surface is already covered by the first layer. Thus, at this stage the growth seems to follow the 2D layer-by-layer mode. However, when occupation of the second layer exceeds 20%, nucleation of the third-layer islands takes place (Fig. 7a), rapidly followed then by nucleation of the forth-layer islands (Fig. 7b). Thus, the growth mode changes to the 3D multi-layer one. Each time, the next-layer islands nucleate preferentially where the atomic steps of the underlying Au/Si(111) substrate are situated. One can see that the step is inherited in the C_{70} molecular layers with a progressive smearing with each next layer. The third-layer islands appear as single molecular sheets that are spread over the step and cover both terraces. The forth-layer islands typically contain screw dislocations. As for the superstructure of the C_{70} layers, one can see that the traces of the 1B2D superstructure of the first layer can be noticed in the next layers, though it concerns mainly the motifs of the superbright fullerenes. Note that a similar inheritance of the first-layer superstructure in the next layers were observed with the C_{60} fullerenes [14], though for a different origin of the superstructure. In the present case, the superstructure in the first layer is associated with a different orientation of elongated C_{70} molecules, hence a similar STM contrast of all molecules in the third and forth layers implies that they are plausibly in the same orientation, namely oriented upright.

4. Conclusions

In conclusion, self-assembly of C_{70} fullerenes adsorbed onto the In- and Tl-modified Si(111)$\sqrt{3} \times \sqrt{3}$-Au surfaces at RT and 112 K has been studied. As compared to the C_{60} fullerenes on the same surfaces, the difference in the behavior of C_{70}s stems from it non-spherical shape and a greater C_{70}-C_{70} bonding. At 112 K, C_{70}s tend to form chain-like islands built of double or triple molecular rows along the [$\bar{1}$10] Si(111) substrate directions, while the C_{70} arrays formed at RT exhibit a stripe-like 3 × 1 reconstruction where a single row of bright fullerenes mediated by double row of dim fullerenes. The reconstruction does not relate to the structure of the underlying Au/Si(111) substrate and originates from the different orientations of C_{70}s within the layer. As a result, the reconstruction does not cause any island size selection that is in contrast to the hexagonal reconstructions of C_{60}s where the bright fullerenes occupying the specific adsorption sites control formation of the magic-size islands.

Acknowledgments

The work was supported by Russian Science Foundation under Grant no. 14-12-00482.

References

[1] K. Pussi, H.I. Li, H. Shin, L.N. Serkovic Loli, A.K. Shukla, J. Ledieu, V. Fournée, L.L. Wang, S.Y. Su, K.E. Marino, M.V. Snyder, R.D. Diehl, Elucidating the dynamical equilibrium of C_{60} molecules on Ag(111), Phys. Rev. B 86 (2012) 205406.
[2] H.I. Li, G.J.P. Abreu, A.K. Shukla, V. Fournée, J. Ledieu, L.N. Serkovic Loli, S.E. Rauterkus, M.V. Snyder, S.Y. Su, K.E. Marino, R.D. Diehl, Ordering and dynamical properties of superbright C_{60} molecules on Ag(111), Phys. Rev. B 89 (2014) 085428.
[3] W. Pai, C.-L. Hsu, Ordering of an incommensurate molecular layer with adsorbate-induced reconstruction: C_{60}/Ag(100), Phys. Rev. B 68 (2003) 121403(R).
[4] C.-L. Hsu, W. Pai, Aperiodic incommensurate phase of a C_{60} monolayer on Ag(100), Phys. Rev. B 68 (2003) 245414.
[5] X. Zhang, W. He, A. Zhao, H. Li, L. Chen, W. Pai, J. Hou, M. Loy, J. Yang, X. Xiao, Geometric and electronic structure of a C_{60} monolayer on Ag(100), Phys. Rev. B 75 (2007) 235444.
[6] J.A. Gardener, G.A.D. Briggs, M.R. Castell, Scanning tunneling microscopy studies of C_{60} monolayers on Au(111), Phys. Rev. B 80 (2009) 235434.
[7] L. Tang, Y. Xie, Q. Guo, Complex orientational ordering of C_{60} molecules on Au(111), J. Chem. Phys. 135 (2011) 114702.
[8] H. Shin, A. Schwarze, R.D. Diehl, K. Pussi, A. Colombier, É Gaudry, G.M. McGuirk, L.N. Serkovic Loli, V. Fournée, L.L. Wang, G. Schull, R. Berndt, Structure and dynamics of C_{60} molecules on Au(111), Phys. Rev. B 89 (2014) 245428.
[9] M. Paßens, S. Karthäuser, Interfacial and intermolecular interactions determining the rotational orientation C_{60} adsorbed on Au(111), Surf. Sci. 642 (2015) 11.
[10] W. Pai, C.-L. Hsu, M. Lin, K. Lin, T. Tang, Structural relaxation of adlayers in the presence of adsorbate-induced reconstruction: C_{60}/Cu(111), Phys. Rev. B 69 (2004) 125405.
[11] S.-S. Wong, W.W. Pai, C.-H. Chen, M.-T. Lin, Coverage-dependent adsorption superstructure transition of C_{60}/Cu(001), Phys. Rev. B 82 (2010) 125442.
[12] T. Nakayama, J. Onoe, K. Takeuchi, M. Aono, Weakly bound and strained C_{60} monolayer on the Si(111)$\sqrt{3} \times \sqrt{3}R30°$-Ag substrate surface, Phys. Rev. B 59 (1999) 12627.
[13] D.V. Gruznev, A.V. Matetskiy, L.V. Bondarenko, A.V. Zotov, A.A. Saranin, J.P. Chou, C.M. Wei, Y.L. Wang, Dim C_{60} fullerenes on Si(111)$\sqrt{3} \times \sqrt{3}$-Ag surface, Surf. Sci. 612 (2013) 31.
[14] A.V. Matetskiy, D.V. Gruznev, A.V. Zotov, A.A. Saranin, Modulated C_{60} monolayers on Si(111)$\sqrt{3} \times \sqrt{3}$-Au reconstructions, Phys. Rev. B 83 (2011) 195421.
[15] D.V. Gruznev, A.V. Matetskiy, L.V. Bondarenko, O.A. Utas, A.V. Zotov, A.A. Saranin, J.P. Chou, C.M. Wei, M.Y. Lai, Y.L. Wang, Stepwise self-assembly of C_{60} mediated by atomic scale moiré magnifiers, Nat. Commun. 4 (2013) 1679.
[16] D.A. Olyanich, V.V. Mararov, T.V. Utas, O.A. Utas, D.V. Gruznev, A.V. Zotov, A.A. Saranin, Magic C_{60} islands forming due to moiré interference between islands and substrate, Surf. Sci. 635 (2015) 94.
[17] T. Nagao, S. Hasegawa, K. Tsuchie, S. Ino, C. Voges, G. Klos, H. Pfnür, M. Henzler, Structural phase transitions of Si(111)-$(\sqrt{3} \times \sqrt{3})R30°$-Au: phase transitions in domain-wall configurations, Phys. Rev. B 57 (1998) 10100.
[18] D.V. Gruznev, I.N. Filippov, D.A. Olyanich, D.N. Chubenko, I.A. Kuyanov, A.A. Saranin, A.V. Zotov, V.G. Lifshits, Si(111)-α-$\sqrt{3} \times \sqrt{3}$-Au phase modified by in adsorption: stabilization of a homogeneous surface by stress relief, Phys. Rev. B 73 (2006) 115335.
[19] J.K. Kim, K.S. Kim, J.L. McChesney, E. Rotenberg, H.N. Hwang, C.C. Hwang, H.W. Yeom, Two-dimensional electron gas formed on the indium-adsorbed Si(111)$\sqrt{3} \times \sqrt{3}$-Au surface, Phys. Rev. B 80 (2009) 075312.
[20] L.V. Bondarenko, D.V. Gruznev, A.A. Yakovlev, A.Y. Tupchaya, D. Usachov, O. Vilkov, A. Fedorov, D.V. Vyalikh, S.V. Eremeev, E.V. Chulkov, A.V. Zotov, A.A. Saranin, Large spin splitting of metallic surface-state bands at adsorbate-modified gold/silicon surfaces, Sci. Rep. 3 (2013) 1826.
[21] Y.G. Ding, C.T. Chan, K.M. Ho, Theoretical investigation of the structure of the $(\sqrt{3} \times \sqrt{3})R$ 30-Au/Si(111) surface, Surf. Sci. 275 (1992) L691.
[22] P. Wang, H.-J. Zhang, Y.-J. Li, C.-Q. Sheng, Y. Shen, H.-Y. Li, S.-N. Bao, H.-N. Li, Effect of charge transfer on the geometric structure of a C_{70} monolayer on the surface of Ag(111), Phys. Rev. B 85 (2012) 205445.
[23] D.A. Olyanich, V.V. Mararov, T.V. Utas, A.V. Zotov, A.A. Saranin, Adsorption and self-assembly of fullerenes on Si(111)$\sqrt{3} \times \sqrt{3}$-Ag: C_{60} versus C_{70}, Surf. Sci. 653 (2016) 138.
[24] F. Rossel, M. Pivetta, F. Patthey, E. Ćavar, A.P. Seitsonen, W.-D. Schneider, Growth and characterization of fullerene nanocrystals on NaCl/Au(111), Phys. Rev. B 84 (2011) 075426.
[25] J.G. Amar, F. Family, P.M. Lam, Dinamic scaling of the island -size distribution and percolation in a model of submonolayer molecular-beam epitaxy, Phys. Rev. B 50 (1994) 8781.

[26] J. Amar, F. Family, Critical cluster size: island morphology and size distribution in submonolayer epitaxial growth, Phys. Rev. Lett. 74 (1995) 2066.

[27] A.V. Matetskiy, L.V. Bondarenko, D.V. Gruznev, A.V. Zotov, A.A. Saranin, J.P. Chou, C.R. Hsing, C.M. Wei, Y.L. Wang, Peculiar diffusion of C_{60} on In-adsorbed Si(111)$\sqrt{3} \times \sqrt{3}$-Au surface, Surf. Sci. 616 (2013) 44.

[28] N.V. Sibirev, V.G. Dubrovskii, A.V. Matetskiy, L.V. Bondarenko, D.V. Gruznev, A.V. Zotov, A.A. Saranin, Size distribution of fullerene surface clusters, Appl. Surf. Sci. 307 (2014) 46.

[29] F. Loske, J. Lübbe, J. Schütte, M. Reichling, A. Kühnle, Quantitative description of C_{60} diffusion on an insulating surface, Phys. Rev. B 82 (2010) 155428.

[30] M.A. Groce, B.R. Conrad, W.G. Cullen, A. Pimpinelli, E.D. Williams, T.L. Einstein, Temperature-dependent nucleation and capture-zone scaling of C_{60} on silicon oxide, Surf. Sci. 606 (2012) 53.